J Fluoresc (2015) 25:1559–1566
DOI 10.1007/s10895-015-1637-7

SHORT COMMUNICATION

A Successful Attempt to Obtain the Linear Dependence Between One-Photon and Two-Photon Spectral Properties and Hammett Parameters of Various Aromatic Substituents in New π-Extended Asymmetric Organic Chromophores

Nvdan Hu[1,2] · Yulong Gong[1] · Xinchao Wang[1] · Yao Lu[1] · Guangyue Peng[1] · Long Yang[1] · Shengtao Zhang[1] · Ziping Luo[1] · Hongru Li[1] · Fang Gao[1]

Received: 18 March 2015 / Accepted: 3 August 2015 / Published online: 7 September 2015

Abstract A series of new asymmetric chromophores containing aromatic substituents and possessing the excellent π-extension in space were prepared through multi-steps routes. One-photon and two-photon spectral properties of these new chromophores could be tuned by these substituents finely and simultaneously. The linear correlation of the wave numbers of the one-photon absorption and emission maxima to Hammett parameters of these substituents was presented. Near infrared two-photon absorption emission integrated areas of the target chromophores were correlated linearly to Hammett constants of these substituted groups.

Keywords One-photon and two-photon spectra · Hammett parameter · Organic chromophore

Electronic supplementary material The online version of this article (doi:10.1007/s10895-015-1637-7) contains supplementary material, which is available to authorized users.

✉ Ziping Luo
zpluo@126.com

✉ Hongru Li
hongruli1972@gmail.com

✉ Fang Gao
fanggao1971@gmail.com

[1] College of Chemistry and Chemical Engineering, Chongqing University, Chongqing, China

[2] School of Pharmaceutical Engineering, Guizhou Institute of Technology, Guiyang 550003, Guizhou, China

Introduction

Organic chromophores with two-photon absorption (TPA) properties receive considerable attentions due to the great application potentials in various fields such as two-photon imaging [1, 2], two-photon data storage [3, 4] and two-photon sensors [5, 6]. Furthermore, two-photon properties of organic photosensitizers make it feasible to perform two-photon photodynamic therapy (PDT) by near-infrared (near-IR) laser [7, 8], which possesses various advantages such as low energy, deep penetration and negligible damage to the normal life cells.

TPA properties of the organic chromophores can be altered by varying the electron-donating/withdrawing substituents or the structures, which influences the ground and excited states of the target molecules. As a result, the introduction of various substituted groups or the construction of branched structures was utilized to increase TPA cross sections of the target molecules [9, 10]. However, because there is great difference between one-photon excitation and two-photon excitation, it is still a great challenge to tune finely one-photon absorption (OPA) and TPA optical properties of new organic chromophores. This means that the ground and excited states of the organic chromophores must be tuned subtly and simultaneously. Hammett parameters (σ) of the various substituents play significant roles in the interpretation and prediction of the electron-donating/withdrawing effect of the substituents [11, 12]. So, the finely tuning the ground and excited states of the organic chromophores means that it is possible to obtain the linear correlation between one-/two-photon spectral properties and Hammett parameters of the substituents.

It is well-accepted that the aromatic substituents affect the molecular geometry of the organic chromophores more greatly than the smaller substituents such as cyano and nitro groups. Hence, it is not easy to establish a linear correlation

between one-/two-photon optical properties and Hammett parameters of aromatic substituents. So far, only few successful efforts on the linear correlation two-photon optical properties to Hammett constants of the large aromatic substituents in porphyrins were reported [13, 14]. It is considered that the entire molecular geometry of porphyrins cannot be altered greatly by the aromatic substituents because the porphyrin molecular structure is symmetric, coplanar and robust. This in turn suggests that it is more difficult to achieve the linear correlation between one-/two-photon optical properties and Hammett parameters of the aromatic substituents in asymmetric fluorescent chromophores.

This communication proposes that if an asymmetric chromophore with great π extension in three-dimensional space is chosen as the parent central core, the aromatic subsituents could not lead to the remarkable alteration on the entire molecular geometry. Thus, to this organic molecule, the intramolecular charge transfer can be the main factor association with one-photon spectral and two-photon optical properties. As a consequence, the linear interrelationship between one-/two-photon spectral properties and Hammett constants of the large aromatic substituents in some asymmetric molecules could be realized.

It is well-known that triphenylamine and diphenylketone display the excellent geometry extension in space, and they are used widely in various fields such as non-linear optical, optoelectronic and photopolymer materials [15, 16]. In this work, the π-extended triphenylamine-based organic chromophore containing phenyl keto segment was utilized as the parent core. 4-Nitro-phenyl, 3-nitro-phenyl, phenyl, 4-methyl-phenyl, phenylethyleneyl and 4-methoxy-phenyl were attached separately to the core to prepare the target chromophores.

This work presented firstly the linear interrelationship between one-/two- photon optical properties and Hammett constants of the large aromatic substituents of these new organic chromophores. The molecular geometry optimization computation revealed preliminarily the fundamental reason on the linear correlation.

Experimental

Reagents and Materials

The commercially available organic solvents were further purified by the standard methods [17]. The new asymmetric organic chromophores (C1~C6) were shown in Scheme 1, in which C1 is 4-nitro-phenyl-phenyl-4′-((4′)’-phenyl-benzoyl-phenylethyleneyl-phenyl)-4″-phenyl-amine, C2 shows 3-nitro-phenyl-phenyl-4′-((4′)’ -phenyl-benzoyl-phenylethylene-yl-phenyl)-4″-phenyl-amine, C3 is 4-phenyl-phenyl-4′-((4′)’-(phenyl-benzoyl-phenylethylene-yl)-phenyl)-4″-phenyl-amine, C4 denotes 4-methyl-phenyl-phenyl-4′-((4′)’-phenyl-benzoyl-phenylethylene-yl-phenyl)-4″-phenyl-amine, C5 represents 4-phenyl-ethyleneyl-phenyl-4′-((4′)’-(phenyl-benzoyl -phenylethylene-yl)-phenyl)-4″-phenyl-amine and C6 shows 4-methoxy-phenyl-phenyl-4′-((4′)’-phenyl-benzoyl-phenylethylene-yl- -phenyl)-4″-phenyl-amine. The new chromophores were synthesized through multi-step routs shown in Scheme 1. The preparation detail of the precursors and the target molecules were provided in the Supplementary Materials.

Chemical Structural Characterization

Bruker 400 and 500 MHz nuclear magnetic resonance (NMR) apparatus were employed to determine the ^{1}H & ^{13}C NMR spectra of the precursors and target molecules in deuterated solvents at room temperature. The ^{1}H & ^{13}C chemical shifts in NMR spectra were measured by using tetramethylsilane (TMS) as the internal standard. The elemental analysis was obtained by CE440 elemental analysis meter obtained from Exeter Analytical Inc. The melting points of the target molecules were detected by Beijing Fukai melting point apparatus.

One-Photon Spectral and Two-Photon Spectral Measurements

The UV/visible absorption spectra of the samples were measured by a TU1901 spectrophotometer of Beijing PUXI General Equipment Limited Corporation, while the one-photon emission spectra were determined by Shimadzu RF-531PC fluorophotonmeter. Rodamin 6G in ethanol (Φ, 0.94) was used as the reference to measure the fluorescence quantum yields of the samples [18]. The optical density at the excited wavelength for the determination of the fluorescence quantum yields of the samples was below 0.1 in order to remove self-quenching of fluorescence emission. The fluorescence quantum yields of the samples were calculated based on the following equation [19]

$$\Phi_f = \Phi_f^0 \frac{n_0^2 A_0 \int I_f(\lambda_f)\mathrm{d}\lambda_f}{n^2 A \int I_f^0(\lambda_f)\mathrm{d}\lambda_f} \quad (1)$$

wherein n_0 and n show the refractive indices of the solvents, A_0 and A represent the optical densities at excitation wavelength, Φ_f and Φ_f^0 are the fluorescence quantum yields, and the integrals are the fluorescence emission spectral areas of the reference and the sample respectively.

The two-photon excited fluorescence spectra of the target molecules were performed by the pumped Ti:sapphire femtosecond laser (Spectra-Physics Ltd., Tsunami mode-locked, 80 MHz, <130 fs, average power ≤700 mW) in the range of 700~880 nm, and the spectra were recorded by Ocean Optics USB2000 CCD camera with the detecting range of 180 to 880 nm. The TPA cross-section (σ) was determined by up-

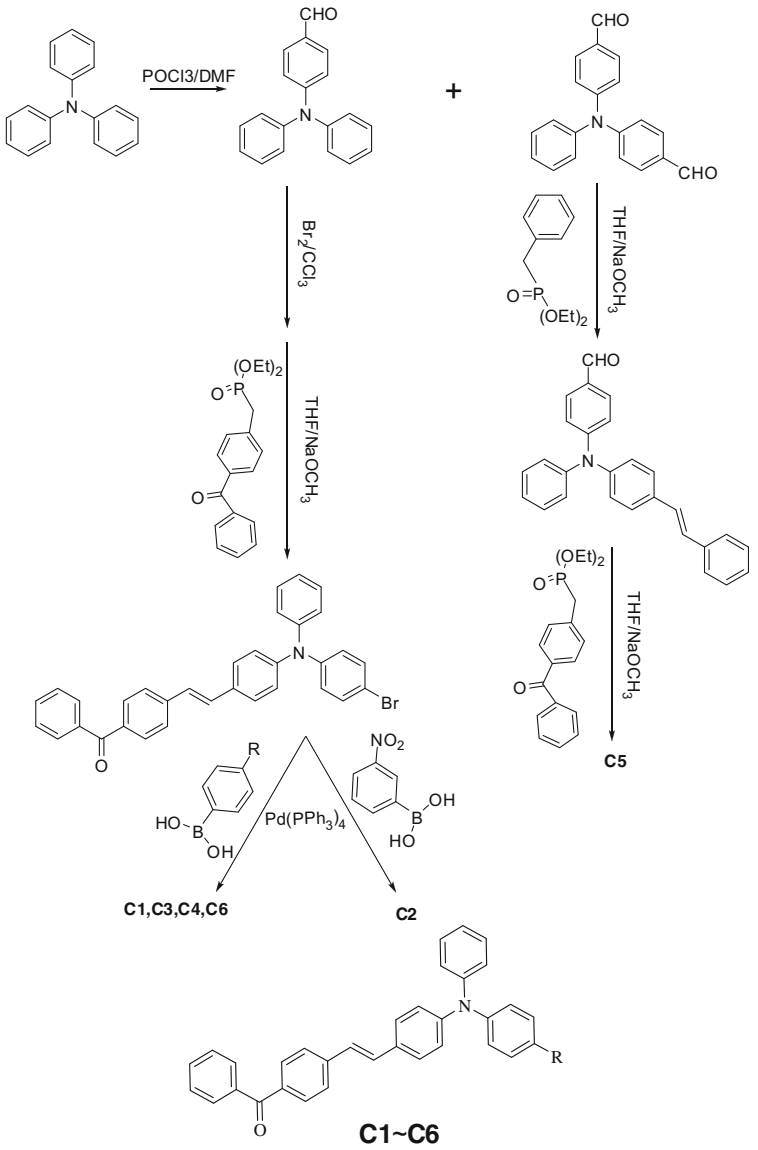

R: **C1**, 4-nitro-phenyl, **C2**, 3-nitro-phenyl, **C3**, phenyl, **C4**, 4-methyl-phenyl, **C5**, phenylethyleneyl, **C6**, 4-methoxy-phenyl

Scheme 1 Synthetic routes of the target molecules C1 to C6

conversed fluorescence method by using 5×10^{-4} mol/L fluorescein in 0.1 mol/L NaOH solution as the reference sample [20]. The all determined samples were bubbled by nitrogen gas for 15 min to remove oxygen molecules before the measurements. The TPA cross sections of the samples were calculated by the following equations [21]:

$$\sigma = \frac{\sigma^{TPE}}{\Phi_F} \tag{2}$$

$$\sigma^{TPE} = \sigma_{cal}^{TPE}\frac{c_{cal}}{c}\frac{n_{cal}}{n}\frac{S}{S_{cal}} \tag{3}$$

wherein σ is the TPA cross sections, σ^{TPE} represents the two-photon excited cross sections, c denotes the concentration of reference and sample molecules, n is the refractive index of the solvents, and S shows the integration areas of two-photon up-converted fluorescence spectra of the sample molecules, cal is used as the reference.

Molecular Geometry Optimization

The molecular geometry optimization was performed by Gaussian 09 program package. The geometry optimization in the ground electronic state (S_0) was carried out by HF level (Hatree-Fock) basing on the B3LYP method [22–24], while the geometry optimization in the excited electronic state (S_1)

was done by CIS (configuration interaction single exCitation) method [25]. Benzene was adopted as the organic solvent.

The energies of the geometries in S_0 or S_1 states of the target molecules were commutated by DFT//HF or TDDFT//CIS correspondingly (wherein the method represents single point calculation //optimization method, DFT is density functional theory, and TDDFT is time-dependence density functional theory).

Results and Discussion

Correlation Between One-Photon Optical Properties and Hammett Constants

OPA spectral properties of the target chromophores were determined in various solvents. It was noticed that the absorption and emission maxima of the target chromophores were red-shifted greatly in strong polar solvents (such as the emission maxima of C1, in benzene, 478 nm, in THF, 519 nm, Table 1, Figure S1, Supplementary materials). The results suggest that the maximal absorption and emission peaks of the target molecules were from the intramolecular charge transfer [26].

It is well-known that the increase in Hammett constant (σ) of a substituted group shows that its electron-accepting ability increases. In other words, the decrease in Hammett constant of the substituent means the increase in its electron-donating strength. Hammett constants of 4-nitro-phenyl, 3-nitro-phenyl, phenyl, 4-methyl-phenyl, phenyl-ethyleneyl and 4-methoxy-phenyl groups are 0.26, 0.20, −0.01, −0.03 −0.07 and −0.08 correspondingly [27]. These parameters show that 4-nitro-phenyl and 3-nitro-phenyl groups display greater electron-accepting nature than the other substituents, while phenylethyleneyl and 4-methoxy-phenyl groups possess more electron-donating ability than phenyl and 4-methyl-phenyl groups. The spectral determination showed that normalized OPA absorption and emission maxima showed the red-shift with the increase in the electron-donating of aromatic substituents (normalized spectra are shown in Fig. 1, also can see the actual spectra in Figure S2). This further demonstrated that OPA absorption and emission maxima of the target chromophores were from the intramolecular charge transfer.

Because the electron-withdrawing or donating ability of the substituent can be shown by its Hammett constant, we analyzed the correlation of OPA spectral properties of the target molecules to Hammett parameters of the aromatic substituents. Plots of the wave numbers of one-photon absorption and emission maxima to Hammett constants of the substituents in the target chromophores in various solvents are given in Fig. 2. The linear plots demonstrate that the properties of the ground state and excited state are shown the remarkable dependence on the electron-donating/accepting properties of aromatic substitutents in the target chromophores. The linear plots indicate that HOMO-LUMO energy gaps of the target chromophores could be correlated to Hammett constants of the aromatic subsituents linearly in both the ground and excited states. Figure 2 shows that the maximal OPA absorption and emission wavelength maxima of the target chromophores exhibited the bathchromic shift with the diminishment of Hammett constants of the aromatic substituents.

Table 1 The spectral parameters of the target molecules in various solvents, $\lambda_{a,max}$: the absorption maximum, nm, $\lambda_{f,max}$: the emission maximum, nm. ε_{max}, the maximal molar coefficient extinction, $mol^{-1}\bullet cm^2$, Φ, the fluorescence quantum yields

Chromophores		Solvents				
		Benzene	THF	CH_2Cl_2	CH_3CN	σ_p
C1	10^{-5} ε	0.376	0.432	0.480	0.443	0.26
	$\lambda_{a\ max}$	389.1	390.5	392.9	396.8	
	Φ	0.125	0.113	0.101	weak	
	$\lambda_{f,max}$	478	519	529	546	
C2	10^{-5} ε	0.148	0.274	0.367	0.2	0.20
	$\lambda_{a\ max}$	394.5	395.8	396.2	401.2	
	Φ	0.175	0.168	0.170	weak	
	$\lambda_{f,max}$	485	532	540	559	
C3	10^{-5} ε	0.371	0.388	0.342	0.361	−0.01
	$\lambda_{a\ max}$	403.8	406.1	408.9	412.2	
	Φ	0.351	0.243	0.092	weak	
	$\lambda_{f,max}$	497	544	552	571	
C4	10^{-5} ε	0.269	0.301	0.356	0.316	−0.03
	$\lambda_{a\ max}$	407.2	408.8	410.8	414.3	
	Φ	0.321	0.371	0.401	0.335	
	$\lambda_{f,max}$	498	550	560	573	
C5	10^{-5} ε	0.405	0.452	0.477	0.489	−0.07
	$\lambda_{a\ max}$	410.4	412.1	413.2	416.5	
	Φ	0.322	0.248	0.121	weak	
	$\lambda_{f,max}$	500	553	561	576	
C6	10^{-5} ε	0.331	0.358	0.383	0.429	−0.08
	$\lambda_{a\ max}$	411.2	413.9	416.2	419.3	
	Φ	0.184	0.209	weak	weak	
	$\lambda_{f,max}$	502	557	564	577	

It is accepted that the intramolecular charge transfer in an organic molecule can be reflected by its dipole moment changes between the ground and excited states. Hence, we further calculated the dipole moment change of the target chromophores based on Lippert equation [28].

$$hc(\nu_{abs}-\nu_{em}) = \frac{2\left(\mu_e-\mu_g\right)^2}{4\pi\varepsilon_0 a^3}\Delta f + const \quad (4)$$

$$\Delta f = \left(\frac{\varepsilon-1}{2\varepsilon+1}-\frac{n^2-1}{2n^2+1}\right) \quad (5)$$

wherein V_{abs} - V_{em} means the Stokes shift, V_{abs}, V_{em} are the wave numbers of the absorption and emission maxima

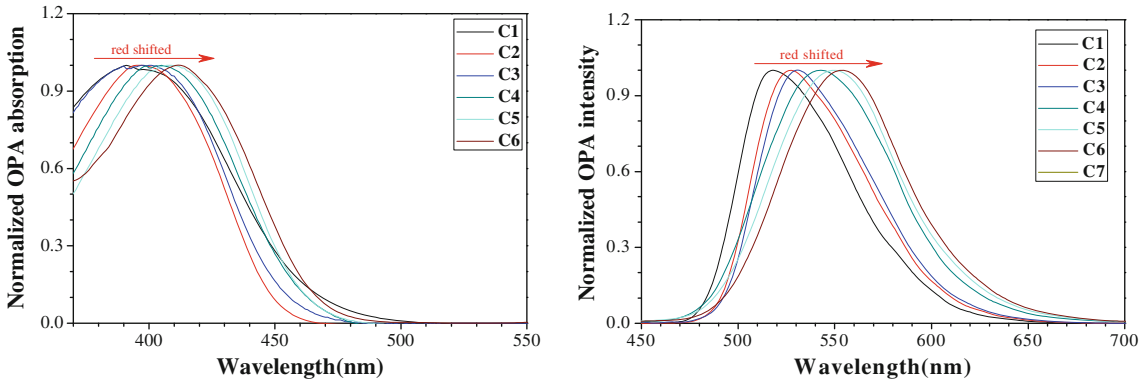

Fig. 1 Normalized OPA absorption and emission spectra of the target chromophores in THF, the absorption, $C=1\times10^{-5}$ mol/L, the emission $C=5\times10^{-6}$ mol/L

respectively. h represents Planck's constant; c shows the speed of light, ε is the static dielectric constant of the solvent, and n is its refractive index; μ_e, μ_g are the permanent dipole moments of the excited and the ground states of the fluorophore respectively; a denotes the radius of the cavity in the solvent to place the fluorophore, Δf is the orientation polazrizability.

The plots of the Stokes shifts to the orientation polarizability (Δf) of solvents for the target chromophores were obtained (figure S3 in Supplementary materials). The line plots suggest that the internal charge transfer plays significant role in the ground and excited states of the target molecules. The results show that the dipole moment change of target molecules increases with the decrease of Hammett constants of the large substituents. (C1, 2.98 debye, C2, 3.50 debye, C3, 5.51 debye, C4, 6.32 debye, C5, 7.29 debye, C6, 7.51 debye). It demonstrates that intramolecular charge transfer in the excited state of the target chromophores is improved by the electron-donating properties of aromatic substituents. These results are interpreted that OPA absorption and emission maxima of C1 and C2 were remarkably blue-shifted comparing with the other target molecules, and the fluorescence quantum yields were lower in various solvents.

Correlation Between Two-Photon Optical Properties and Hammett Constants

The TPA optical properties of these chromophores were measured by utilizing near-IR Ti:sapphire femtosecond laser tuning the excitation wavelength from 700 to 880 at 20 nm step. The target chromophores showed great TPA upconverted fluorescence emission under near-IR laser excitation (shown typically in Fig. 3). It was observed that TPA emission maxima of the chromophores are irrespective of the excited near-IR laser wavelengths (Table S1, Supplementary material), which suggests that the excited states formed in TPA process was insensitive to near-IR laser excited wavelength. The TPA emission maxima of the target molecules are longer than OPA emission maxima, which can be ascribed to the reabsorption of the shorter wavelengths in the emission spectra [29].

Since the OPA optical properties of C1~C6 are dependent on the electron-donating/accepting properties of the aromatic substituents, it is considered that TPA optical nature can be correlated to Hammett constants of these substituted groups as well. While unlike one photon excitation process, the wave numbers of TPA emission maxima of the target chromophores did not exhibit the linear correlation to the Hammett

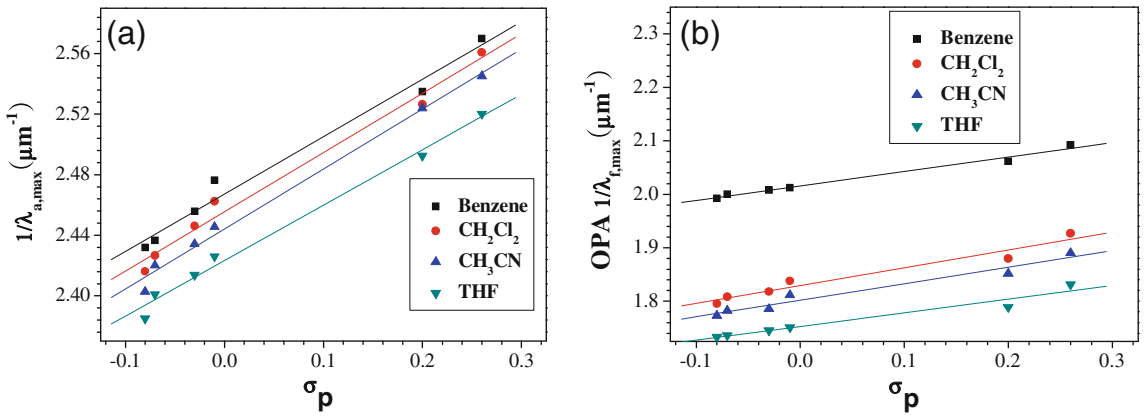

Fig. 2 Plots of the wave-numbers (μm^{-1}) of OPA maxima (**a**) and one-photon fluorescence maxima (**b**) versus Hammett constants of the substituents of C1~C6 in various solvents

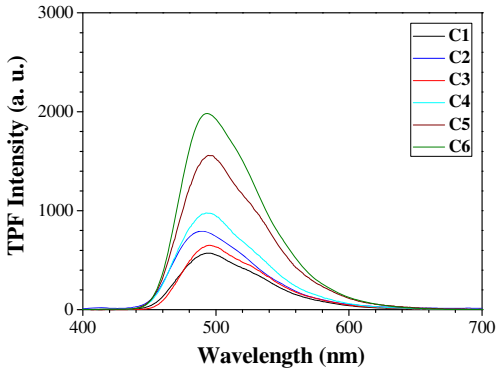

Fig. 3 Typical TPA emission of C1~C6 in benzene under 800 nm femtosecond laser irradiation

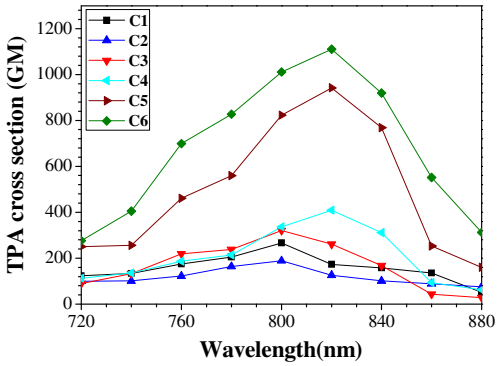

Fig. 5 TPA cross sections of C1~C6 under various excited near-IR wavelength (700~880 nm), 1 GM=10^{-50} cm^4 s/photon

parameters of the aromatic substituents. However, the linear relationship was obtained between Hammett constants of the large aromatic substituents and the TPA emission integrated areas under the same near-IR irradiation (Fig. 4). It indicates that the TPA cross sections of the target molecules were affected greatly by the intramolecular charge transfer effect of these substituents. The negative slopes indicate that the TPA emission integrated areas of C1~C6 increased with the decrease of the electron-accepting ability of the aromatic substituents [30]. The results show that it is the electron-donating/accepting nature that makes the major contribution to TPA optical properties of the target molecules. This is mainly due to the significant influence of the aromatic substituents on the intramolecular charge transfer in the ground and excited states of the target chromophores.

We further determined the TPA cross sections of the molecules according to the TPA fluorescence methods. C6 showed the largest TPA cross sections under the most of near-IR laser wavelength excitation among C1~C6 (~1100 GM at 820 nm, Fig. 5). The electron-withdrawing effect can be the main reason for the smaller TPA cross sections of C1 and C2 comparing with the other molecules.

It is noticed that the TPA emission integrated areas of these molecules under different power near-IR laser followed the square law well, and the slope around 2.00 showed typical TPA process. (shown typically in Figure S4, Supplementary materials).

The molecular geometry optimization was performed to reveal the correlation of OPA and TPA optical properties to Hammett constants of the aromatic substituents. It was found that the geometry of the target molecules exhibited neat space extension. Although the electronic cloud density distribution was mainly distributed around N core of triphenylamine in HOMO to these target molecules, while in LUMOs of the target chromophores without nitro group, the electronic cloud density were mainly located at the branch containing carbonyl group. The electronic cloud density distribution in LUMOs of C1 and C2 is different from that of the other chromophores, indicating the properties of the frontier orbitals can be altered by the aromatic subsitutents. (figure S5, Supplementary materials).

The energy level of HOMO and LUMO, and the energy gaps of HOMO-LUMO gaps showed linear correlation to the Hammett parameters of the substituents (Fig. 6). It is interpreted as the linear correlation between the wave-numbers of one-photon absorption and emission maxima of the target molecules to Hammett parameters of the substituents. Figure 6 indicates that the HOMO-LUMO gaps of the target chromophores increased with enhancement of the electron-accepting strength of the

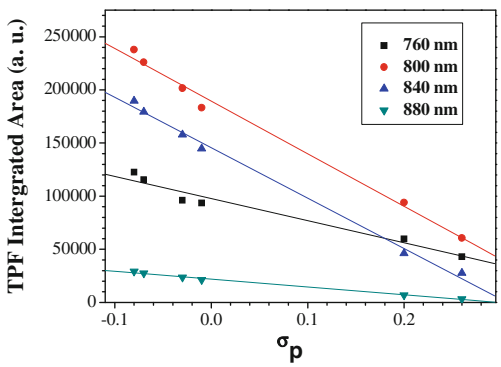

Fig. 4 Plots of TPA emission integrated areas of C1~C6 to Hammett constants of the substituents under various near-IR laser wavelength excitation in benzene

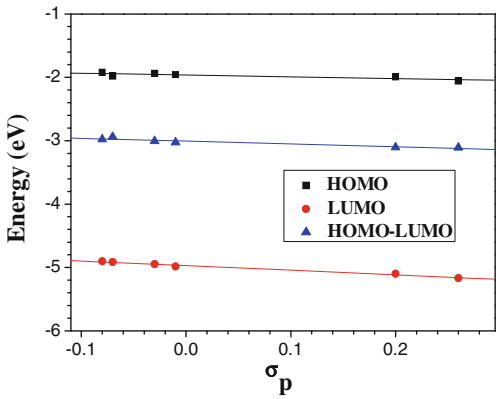

Fig. 6 Plots of the orbital energy levels (HOMO and LUMO) of C1~C6 to Hammett constants (σ_p)

substituents. In other words, the HOMO-LUMO gaps of the target molecules lowered with the increase of the electron-donating effect of the substituents. Therefore, the OPA absorption and emission maxima of the target chromophores were shifted hypsochromically with the increase of electron-withdrawing ability of the large substituents.

The edge-to-face interactions for either axially or facially substituted benzenes are theoretically studied, which shows that the effect of the small substitutes (NO_2, CN, Br, Cl, F) on the aromatic ring could be very complex [31]. The first one is in the case of axially substituted aromatic systems, the electron density at the para position is considered as a significant stabilizing factor. As a consequence, the stabilization/destabilization by substitution is highly correlated to the electrostatic energy, and in the subsequent correlation with the polarization and charge transfer. The other cases are the facially substituted aromatic system depends on not only the electron-donating ability responsible for the electrostatic energy but also the dispersion interaction and exchange repulsion.

To our work, the target molecules are much similar to the first case one that the para-aromatic substitution plays the important role in the stabilizing molecular geometry, and finally the polarization and charge transfer could be much related to Hamment constants of these aromatic substitutes. Since our target molecules possess much greater chemical size, and the π-extension of these target molecules is more remarkable, the substitution effect could be correlated to the π-aggregation. In order to confirm the aggregation effect in the common pure organic solvents, we did the determination in lower concentration (10^{-7} mol/L) and higher concentration as (10^{-4}~10^{-3} mol/L) of these target molecules. However, the results are consistent with those mentioned above surveyed in this work. As a matter of the fact, the only addition of the insoluble water to organic solvents, the nano π-aggregation could be formed [32]. In our further experiments, the nano aggregation of the target molecules could be formed in binary solvents such as DMF/H_2O or MeOH/H_2O. But in pure organic solvents, none of nano aggregation could be obtained. Additionally, the aggregation size and shape did not exhibit significant variation with these aromatic subsitutents. All the aggregation of the target molecules shows the cubic shape with ~500 nm. This shows that the experimental results in pure organic solvents in our manuscript are not related to the π-aggregation. Although the intramolecular charge transfer effect of the aromatic substitutes could be indirectly indication, it is more reasonable to explain the experimental phenomena in this work.

Conclusions

In this work, the linear correlation of OPA and TPA spectral properties to Hammett constants of the large aromatic substituents in π-extended asymmetric was achieved at the same time firstly. These results also demonstrate that a fully π-extended geometry in three dimensional space is favorable for tuning finely the ground and excited states of the asymmetric chromospheres by varying the large size electron donating/accepting substituents. The results suggest that the electron-donating/withdrawing effect of the substituents plays the key roles in the OPA and TPA optical properties to these chromophores. It was further confirmed by the linear correlation of the energies of HOMO, LUMO and HOMO-LUMO energy gaps to Hammett parameters of the large substituents.

To be summarized, the OPA and TPA spectral properties in these new asymmetric chromophores can be tuned efficiently by varying the electron donating/withdrawing substituted groups. The results presented in this work would be greatly beneficial for the preparation of various functional π-extended asymmetric chromophores with large TPA cross sections in the future.

Acknowledgments This work was finically supported by chongqing natural science foundation projects CSTC2012JJB50007 and CSTC2010BB0216. H. Li is grateful to the Postdoctoral Science Foundation of China for their encouraging supporting (Grants 22012T50762 & 2011M501388). We greatly appreciate Key Laboratory of Photochemical Conversion and Optoelectronic Materials, CAS for the help in the laser detection.

References

1. Taki M, Wolford JL, O'Halloran TV (2004) Emission ratiometric imaging of intracellular zinc: design of a benzoxazole fluorescent sensor and its application in two-photon microscopy. J Am Chem Soc 126(3):712–713
2. Kreisel D, Nava RG, Li W, Zinselmeyer BH, Wang B, Lai J, Pless R, Gelman AE, Krupnick AS, Miller MJ (2010) In vivo two-photon imaging reveals monocyte-dependent neutrophil extravasation during pulmonary inflammation. Proc Natl Acad Sci U S A 107(42): 18073–18078
3. Belfield KD, Schafer KJ (2002) A new photosensitive polymeric material for WORM optical data storage using multichannel two-photon fluorescence readout. Chem Mater 14(9):3656–3662
4. Nguyen LH, Straub M, Gu M (2005) Acrylate-based photopolymer for two-photon microfabrication and photonic applications. Adv Funct Mater 15(2):209–216
5. Kim HM, Jeong MY, Ahn HC, Jeon SJ, Cho BR (2004) Two-photon sensor for metal ions derived from azacrown ether. J Org Chem 69(17):5749–5751
6. Liu ZQ, Shi M, Li FY, Fang Q, Chen ZH, Yi T, Huang CH (2005) Highly selective two-photon chemosensors for fluoride derived from organic boranes. Org Lett 7(24):5481–5484
7. Kim S, Ohulchanskyy TY, Pudavar HE, Pandey RK, Prasad PN (2007) Organically modified silica nanoparticles co-encapsulating photosensitizing drug and aggregation-enhanced two-photon absorbing fluorescent dye aggregates for two-photon photodynamic therapy. J Am Chem Soc 129(9):2669–2675
8. Gary-Bobo M, Mir Y, Rouxel C, Brevet D, Basile I, Maynadier M, Vaillant O, Mongin O, Blanchard-Desce M, Morère A, Garcia M, Durand J-O, Raehm L (2011) Mannose-functionalized mesoporous

silica nanoparticles for efficient two-photon photodynamic therapy of solid tumors. Angew Chem Int Ed 50(49):11425–11631
9. Lee SK, Yang WJ, Choi JJ, Kim CH, Joen SJ, Cho BR (2005) 2,6-Bis[4-(p-dihexylaminostyryl)styryl]anthracene derivatives with large two-photon cross sections. Org Lett 7(2):323–326
10. Strehmel B, Sarker AM, Detert H (2003) The influence of σ and π acceptors on two-photon absorption and solvatochromism of dipolar and quadrupolar unsaturated organic compounds. Chem Phy Chem 4(3):249–259
11. Rogers CJ, Dickerson TJ, Brogan AP, Janda KD (2005) Hammett correlation of nornicotine analogues in the aqueous aldol reaction: implications for green organocatalysis. J Org Chem 70(9):3705–3708
12. Brink BD, DeFrancisco JR, Hillner JA, Linton BR (2011) Curtin–hammett and steric effects in HOBt acylation regiochemistry. J Org Chem 76(13):5258–5263
13. Antonov L, Kamada K, Ohta K, Kamounah FS (2003) A systematic femtosecond study on the two-photon absorbing D-π-A molecules–π-bridge nitrogen insertion and strength of the donor and acceptor groups. Phys Chem Chem Phys 5:1193–1197
14. Drobizhev M, Makarov NS, Stepanenko Y, Rebane A (2006) Near-infrared two-photon absorption in phthalocyanines: enhancement of lowest gerade-gerade transition by symmetrical electron-accepting substitution. J Chem Phys 124:224701
15. Li JY, Li Q, Liu D (2011) Novel Thieno-[3,4-b]-Pyrazines cored dendrimers with carbazole dendrons: design, synthesis, and application in solution-processed red organic light-emitting diodes. ACS Appl Mater Int 3(6):2099–2107
16. Huang LT, Yen HJ, Liou GS (2011) Substituent effect on electrochemical and electrochromic behaviors of ambipolar aromatic polyimides based on aniline derivatives. Macromolecules 44(24):9595–9610
17. Perrin D, Armarego W, Perrin D (1966) Purification of laboratory chemicals. Pergamon, New York
18. Fischer M, Georges J (1996) Fluorescence quantum yield of rhodamine 6G in ethanol as a function of concentration using thermal lens spectrometry. Chem Phys Lett 260(1–2):115–118
19. Maus M, Rettig W (1999) Photoinduced intramolecular charge transfer in a series of differently twisted donor-acceptor biphenyls as revealed by fluorescence. J Phys Chem A 103(18):3388–3401
20. Xu C, Webb WW (1996) Measurement of two-photon excitation cross sections of molecular fluorophores with data from 690 to 1050 nm. J Opt Soc Am B 13(3):481–491
21. Albota MA, Xu C, Webb WW (1998) Two-photon fluorescence excitation cross sections of biomolecular probes from 690 to 960 nm. Appl Opt 37(31):7352–7356
22. Zgiershi MZ, Grabowska A (2000) Photochromism of Salicylideneaniline (SA). How the photochromic transient is created: a theoretical approach. J Chem Phys 12(14):6329–6338
23. Yi PG, Liang YH, Cao CZ (2005) Intramolecular proton or hydrogen-atom transfer in the ground and excited-states of 2-hydroxybenzophenone: a theoretical study. Chem Phys 315(3):297–302
24. Liang YH, Yi PG (2007) Theoretical studies on structure, energetic and intramolecular proton transfer of Alkannin. Chem Phys Lett 438(4–6):173–177
25. Yang ZN, Yang SY, Zhang JP (2007) Ground-and excited-state proton transfer and rotamerism in 2-(2-Hydroxyphenyl)-5-Phenyl-1, 3, 4-Oxadiazole and its O/"NH or S"-substituted derivatives. J Phys Chem A 111(28):6354–6360
26. Iyoda M, Nakamura N, Todaka M, Ohtsu S, Hara K, Kuwatani Y, Yoshida M, Matsuyama H, Sugita M, Tachibana H, Inoue H (2000) Novel synthesis of hexaaryl[3]radialenes via dibromo[3]dendralenes. Tetrahedron Lett 41(36):7059–7064
27. Hansch C, Leo A, Taft RW (1991) A survey of Hammett substituent constants and resonance and field parameters. Chem Rev 91(2):165–195
28. Lippert E (1957) Spektroskopische Bistimmung Des Dipolmomentes Aromatischer Verbindungen im Ersten Angeregten Singulettzustand. Z Electrochem 61:962
29. Kim S, Zheng QD, He GS, Bharali DJ, Pudavar HE, Baev A, Prasad PN (2006) Aggregation-enhanced fluorescence and two-photon absorption in nanoaggregates of a 9,10-Bis[4′-(4″-aminostyryl)styryl]anthracene derivative. Adv Funct Mater 16(18):2317–2323
30. Wan Y, Jia K, Li BS, Bo ZS, Xia AD (2006) Enhancement of two-photon absorption cross-section and singlet-oxygen generation in porphyrins upon β-functionalization with donor − acceptor substituents. Org Lett 8(13):2719–2722
31. Lee EC, Hong BH, Lee JY, Kim JC, Kim D, Kim Y, Kim KS (2005) Substituent effects on the edge-to-face aromatic interactions. J Am Chem Soc 127(12):4530–4537
32. Qian Y, Li S, Zhang G, Wang Q, Wang S, Xu H, Yang G (2007) Aggregation-induced emission enhancement of 2-(2′-hydroxyphenyl) benzothiazole-based excited-state intramolecular proton-transfer compounds. J Phys Chem B 111(21):5861–5868